
Photoluminescence and Energy Transfer Between Sm^{3+} Ions in LaF_3 Nanocrystals Prepared by Hydrothermal Method

Hoang Manh Ha^{1,2,*}, Tran Thi Quynh Hoa^{1,3}, Le Van Vu¹, Nguyen Ngoc Long¹

¹Center for Materials Science, Faculty of Physics, Vietnam National University, Hanoi University of Science, Hanoi, Vietnam

²Department of Physics, Hanoi Architectural University, Hanoi, Vietnam

³Department of Physics, National University of Civil Engineering, Hanoi, Vietnam

Email address:

hoangmanhha@hus.edu.vn (H. M. Ha)

*Corresponding author

To cite this article:

Hoang Manh Ha, Tran Thi Quynh Hoa, Le Van Vu, Nguyen Ngoc Long. Photoluminescence and Energy Transfer Between Sm^{3+} Ions in LaF_3 Nanocrystals Prepared by Hydrothermal Method. *International Journal of Materials Science and Applications*.

Vol. 5, No. 6, 2016, pp. 284-289. doi: 10.11648/j.ijmsa.20160506.18

Received: October 10, 2016; **Accepted:** October 19, 2016; **Published:** November 9, 2016

Abstract: The aim of this research is to study photoluminescent properties and particularly energy transfer between Sm^{3+} ions in LaF_3 nanocrystals because the energy transfer process has a significant effect on the luminescence efficiency and lifetime. Sm^{3+} -doped LaF_3 nanocrystals with 0.1, 0.2, 0.3, 1.0, 2.0, 3.0, 4.0 and 5.0 mol% Sm^{3+} have been prepared by hydrothermal method. The obtained nanocrystals were characterized by X-ray diffraction, transmission electron microscopy, photoluminescence and luminescence decay measurement. The results showed that the $\text{LaF}_3:\text{Sm}^{3+}$ nanocrystals possess hexagonal structure with $P\bar{3}c1$ space group. The room temperature photoluminescence and photoluminescence excitation spectra of $\text{LaF}_3:\text{Sm}^{3+}$ were investigated in detail and interpreted by optical intra-configurational f-f transitions within Sm^{3+} ions. When Sm^{3+} ion concentration in the nanocrystals is increased, the excitation energy is transferred from the “bulk” Sm^{3+} ions to the surface Sm^{3+} ions followed by non-radiative recombination at centers at the surface of the nanocrystals. The photoluminescence decay curves of 593 nm peak in the LaF_3 nanocrystals doped with 1.0-5.0 mol% Sm^{3+} were best fitted to the Inokuti-Hirayama model with the dominant dipole-quadrupole interaction ($S = 8$). The values of fitting parameters for the energy transfer process were determined.

Keywords: $\text{LaF}_3:\text{Sm}^{3+}$ Nanocrystals, Hydrothermal Method, Photoluminescence, Luminescence Decay, Energy Transfer

1. Introduction

The study of rare-earth (RE) fluorides is currently an active research field in materials chemistry because these compounds have potential applications in optics, optoelectronics, biomedicine (e.g. lighting and displays, biological labelling and catalysis fields, etc...). Among RE fluorides, lanthanum trifluoride (LaF_3) is considered as an ideal host material for different luminescent lanthanide ions due to its very low vibrational energies ($\sim 350 \text{ cm}^{-1}$), therefore, the multiphonon relaxation of the excited states of the RE dopant ions will be minimal, resulting in a decrease of the non-radiative rate and a high quantum efficiency of the luminescence.

LaF_3 nanostructures have been synthesized via different

synthetic methods such as hydrothermal [1], solvothermal [2], precipitation [3], sol-gel [4], polyol-mediated [5] and microwave-assisted [6]. LaF_3 nanostructures were formed in different morphology depending on technological conditions. Many authors obtained nanoparticles [1, 4, 6-8], core-shell nanoparticles [3, 8]. Some authors obtained nanoplates [5], while the other one [2] received nanorods.

It is well known that the rare earth doped LaF_3 nanophosphor exhibits efficient room temperature emission from the UV to the mid-IR. LaF_3 host matrix was doped with different RE ions such as Eu^{3+} [3, 7, 8], Nd^{3+} [1, 9], Ce^{3+} [10], Er^{3+} [11] and co-doped with Ce^{3+} and Tb^{3+} [4, 6, 12], Yb^{3+} and Ho^{3+} [13]. It is surprising that Sm^{3+} is one of the most popular RE ions, which is used extensively in optical devices; but in the existing literature, work on the luminescent property of Sm^{3+} ions doped in LaF_3 is

extremely rare.

In our previous work [14], we studied absorption properties and used Judd-Ofelt (J-O) theory for investigating optical properties of Sm^{3+} -doped LaF_3 ($\text{LaF}_3:\text{Sm}^{3+}$) nanocrystals fabricated by hydrothermal method. In this report, we center our attention on the photoluminescence (PL) and photoluminescence excitation (PLE) properties of the $\text{LaF}_3:\text{Sm}^{3+}$ nanocrystals. Especially the excitation energy transfer processes between Sm^{3+} ions in the $\text{LaF}_3:\text{Sm}^{3+}$ nanocrystals have been studied, based on Inokuti-Hirayama model.

2. Experimental Procedures

LaF_3 nanocrystals doped with 0.1, 0.2, 0.3, 1.0, 2.0, 3.0, 4.0 and 5.0 mol% of Sm^{3+} ions were prepared by hydrothermal method. All the chemicals used in our experiment, including lanthanum oxide (La_2O_3), samarium oxide (Sm_2O_3), ammonium fluoride (NH_4F) and glycine ($\text{NH}_2\text{CH}_2\text{COOH}$) are of analytic grade without further purification. In a typical synthesis, 0.977 g of La_2O_3 and 1.046 g Sm_2O_3 were dissolved in dilute HNO_3 , and then dissolved in 48 ml deionized water under stirring, resulting in the formation of a colorless solutions of $\text{La}(\text{NO}_3)_3$ and $\text{Sm}(\text{NO}_3)_3$, respectively. The two mentioned above solutions were mixed in accordance with the appropriate rate. After that, 0.4504 g of glycine was added into the mixture solution with stirring for 30 min to form lanthanum (samarium)-glycine complex. Then, 0.667 g NH_4F was dissolved in 50 ml deionized water and the obtained NH_4F aqueous solution was slowly added dropwise to the above complex solution. After vigorous stirring for 1 h at 50°C , the milky colloidal solution was obtained and poured into a Teflon-lined stainless steel autoclave, and then heated at 150°C for 12 h. After the autoclave was naturally cooled down to room-temperature, the precipitates were collected by centrifugation (6000 rpm) for 20 min and washed with deionized water. This filtering-washing process was repeated 10 times. The final product was dried in air at 60°C for 12 h.

Crystal structure of the synthesized samples was characterized by an X-ray diffractometer SIMEMS D5005, Bruker, Germany with $\text{Cu-K}\alpha_1$ irradiation ($\lambda = 1.54056 \text{ \AA}$). The morphology of the samples was observed by using a transmission electron microscope Tecnai G²20 FEI. Room temperature PL and PLE spectra of the samples were measured on a spectrofluorometer FL 3-22 JobinYvonSpex using 450 W xenon arc lamp as the excitation source. The PL decay curves were measured using a Varian Cary Eclipse Fluorescence Spectrophotometer.

3. Results and Discussion

3.1. Structure and Morphology

X-ray diffraction (XRD) patterns of pure LaF_3 and $\text{LaF}_3:\text{Sm}^{3+}$ nanocrystals are presented in Figure 1.

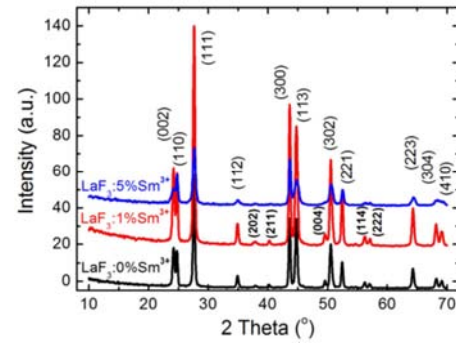


Figure 1. XRD patterns of LaF_3 nanocrystals doped with different Sm^{3+} concentrations.

All the XRD peaks are unambiguously indexed to hexagonal phase with $P\bar{3}c1$ space group of LaF_3 structure (JCPDS card no. 32-0483) with the following diffraction peaks: (002), (110), (111), (112), (202), (211), (300), (113), (004), (302), (221), (114), (222), (223), (304) and (410). No peaks of any other phases or impurities are detected. The lattice parameters were calculated to be $a = 7.172 \pm 0.002 \text{ \AA}$ and $c = 7.342 \pm 0.002 \text{ \AA}$ in good agreement with standard values $a = 7.187 \text{ \AA}$ and $c = 7.350 \text{ \AA}$ (JCPDS card no. 32-0483).

By applying Scherrer's formula $L = 0.9\lambda/(\beta\cos\theta)$ to the (111) diffraction peak, the average crystallite sizes of LaF_3 nanocrystals doped with 0.0, 1.0, 2.0, 3.0, 4.0 and 5.0 mol% Sm^{3+} are estimated to be 27.0, 23.7, 23.6, 16.9, 16.4 and 16.2 nm, respectively.

Figure 2a shows a transmission electron microscopy (TEM) image, Figures 2b and 2c show an enlarged TEM image and the corresponding fast Fourier transformation (FFT) pattern with [0001] zone axis of pure LaF_3 nanocrystals. The measured lattice spacing is 0.36 nm which corresponds to the (110) plane of hexagonal LaF_3 nanocrystals in good agreement with the result of XRD analysis.

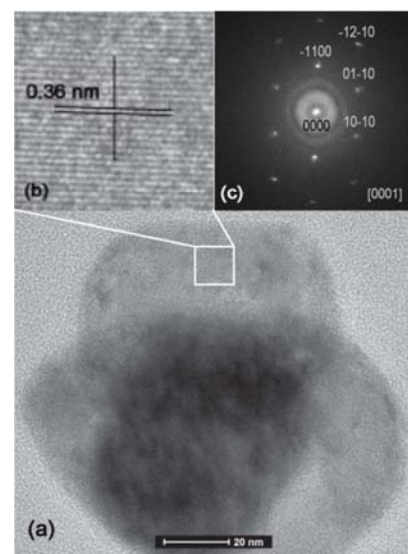


Figure 2. (a) TEM image, (b) Magnified TEM image of area labeled by square in the TEM image and (c) corresponding FFT pattern of LaF_3 nanocrystals.

3.2. Photoluminescence

Typical room-temperature PL spectra of undoped LaF_3 and $\text{LaF}_3:\text{Sm}^{3+}$ nanocrystals doped with 0.3, 1.0, 3.0, and 5.0 mol% Sm^{3+} are shown in Figure 3. As seen from figure, undoped LaF_3 sample does not emit light, whereas $\text{LaF}_3:\text{Sm}^{3+}$ samples exhibit emission spectra with four dominant peaks at 560, 593, 639, and 705 nm corresponding to the emission transitions from the ${}^4\text{G}_{5/2}$ excited state to the ${}^6\text{H}_{5/2}$, ${}^6\text{H}_{7/2}$, ${}^6\text{H}_{9/2}$ and ${}^6\text{H}_{11/2}$ states of the Sm^{3+} ion, respectively. As can be seen from the results of Judd-Ofelt analysis [14], the two transitions ${}^4\text{G}_{5/2} \rightarrow {}^6\text{H}_{9/2}$ and ${}^6\text{H}_{11/2}$ are purely electric-dipole (ED) transitions whereas the other two transitions ${}^4\text{G}_{5/2} \rightarrow {}^6\text{H}_{5/2}$ and ${}^6\text{H}_{7/2}$ contain contributions of both the ED and magnetic-dipole (MD). Additionally, it is found from the inset of Figure 3 that the PL intensity achieved its maximal value for the samples doped with 1 mol% Sm^{3+} . When the Sm^{3+} concentration is higher than 1 mol%, the PL intensity decreased. This is the well-known concentration quenching phenomenon.

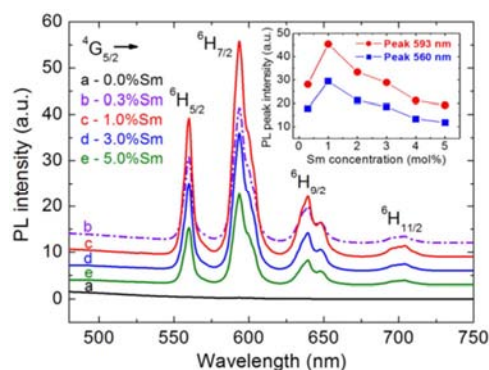


Figure 3. The room-temperature PL spectra under 400 nm excitation of the pure LaF_3 and $\text{LaF}_3:\text{Sm}^{3+}$ nanocrystals doped with different Sm^{3+} concentrations. The inset shows the intensity of emission peaks at 593 and 560 nm as a function of Sm concentration.

It is worth noting that all the emission lines have the same excitation spectra, which proves that all these lines possess the same origin. Typical PLE spectra monitored at 560, 593, and 639 nm emission lines of $\text{LaF}_3:5\%\text{Sm}^{3+}$ nanocrystals are depicted in Figure 4. The absorption spectrum of these nanocrystals is shown as well for comparison.

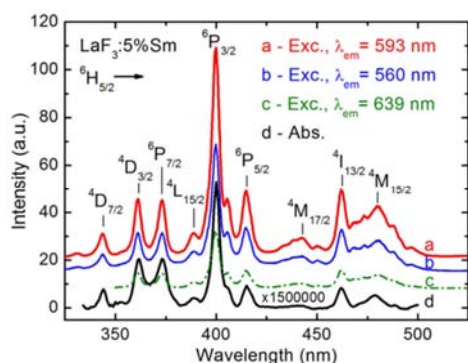


Figure 4. (a, b, c) Room-temperature PLE spectra monitored at 593, 560, and 639 nm emission lines, respectively, of the $\text{LaF}_3:5\%\text{Sm}^{3+}$ nanocrystals and (d) Absorption spectrum of the $\text{LaF}_3:5\%\text{Sm}^{3+}$ nanocrystals.

It is noted that the excitation spectra coincides perfectly with the absorption spectrum and they both exhibit some bands assigned to f-f transitions from the ground state to various excited states of Sm^{3+} ions. Namely, nine of discrete absorption bands located at 344, 362, 373, 389, 400, 415, 443, 462, and 479 nm are assigned to the transitions from the ${}^6\text{H}_{5/2}$ ground state to the ${}^4\text{D}_{7/2}$, ${}^4\text{D}_{3/2}$, ${}^6\text{P}_{7/2}$, ${}^4\text{L}_{15/2}$, ${}^6\text{P}_{3/2}$, ${}^6\text{P}_{5/2}$, ${}^4\text{M}_{17/2}$, ${}^4\text{I}_{13/2}$, and ${}^4\text{M}_{15/2}$ excited states of Sm^{3+} ions, respectively.

Figure 5 shows the simplified energy level diagram of Sm^{3+} ion and the observed excitation and emission transitions in f-f configuration of Sm^{3+} ions.

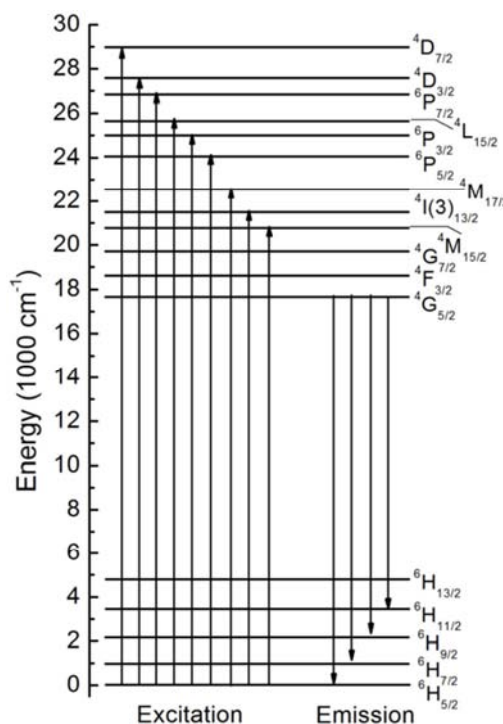


Figure 5. Simplified energy level diagram of Sm^{3+} ion and the observed excitation and emission transitions in $\text{LaF}_3:\text{Sm}^{3+}$ nanocrystals.

3.3. Photoluminescence Decay and Energy Transfer

The PL decay curves for the ${}^4\text{G}_{5/2} \rightarrow {}^6\text{H}_{7/2}$ transition (593 nm) of $\text{LaF}_3:\text{Sm}^{3+}$ nanocrystals with different Sm^{3+} concentrations are presented in Figure 6. As shown in the figure, the PL decay curve of the sample doped with 0.1 mol% Sm^{3+} is found to be perfectly single-exponential with the lifetime of 6.70 ms, while the PL decay curves of the samples doped with 1.0; 3.0; 4.0 and 5.0 mol% Sm^{3+} are non-exponential. In the case of non-exponential decay, the experimental lifetime τ_{exp} of ${}^4\text{G}_{5/2}$ emitting level is determined by taking first e-folding time of the decay curves [15, 16]. The lifetime decreases from 6.70 to 0.75 ms with increasing Sm^{3+} concentration from 0.1 to 5.0 mol%, respectively (Table 1).

The reason for the lifetime decrease is due to the excitation energy transfer process between the optically active ions. When the concentration of RE ions in a solid is low, the interactions between the optically active ions are negligible

and the fluorescence decay curves can be described by a single exponential.

$$C_{DA}^{(S)} = \frac{R_0^S}{\tau_0} \quad (3)$$

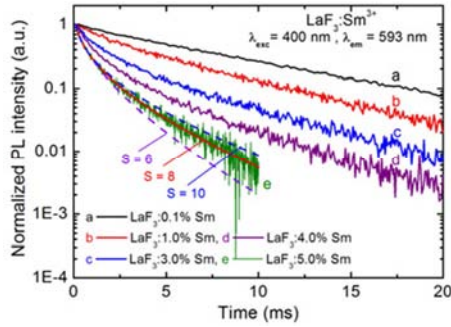


Figure 6. PL decay curves for the ${}^4G_{5/2} \rightarrow {}^6H_{7/2}$ transition (593 nm) of $\text{LaF}_3:\text{Sm}^{3+}$ nanocrystals with different Sm^{3+} concentrations. The IH model fits for $S = 6, 8,$ and 10 are shown for $\text{LaF}_3:5\%\text{Sm}^{3+}$ sample.

Table 1. Lifetime τ_{exp} , energy transfer parameter Q , critical distance R_0 , donor-acceptor interaction parameter C_{DA} ($\times 10^{-56} \text{cm}^8/\text{s}$), energy transfer rate W_{ET} and quantum efficiency η as a function of Sm^{3+} concentration in LaF_3 nanocrystals.

Sm^{3+} concentration (mol%)	Sm^{3+} concentration (10^{20} ions/ cm^3)	τ_{exp} (ms)	Q	R_0 (cm^{-8})	C_{DA}	W_{ET} (s^{-1})	η (%)
0.1	0.05	6.70	-	-	-	-	-
1.0	0.84	4.01	0.30	4.50	0.25	-	-
3.0	1.48	1.80	0.90	5.38	1.05	293	47
4.0	1.97	1.16	1.36	5.60	1.45	402	46
5.0	2.46	0.75	1.92	5.83	2.00	787	41

At high enough concentration of RE ions, the multipolar interactions between the ions sufficiently close to each other are important and the excitation energy can directly transfer from an excited RE ion (or donor ion) to a non-excited RE ion (or acceptor ion), leading to a non-exponential shape for the decay curves and a decrease of lifetime. In this case, according to Inokuti-Hirayama (IH) model [17], the fluorescence decay intensity $I(t)$ can be expressed by the function:

$$I(t) = I_0 \exp \left[-\frac{t}{\tau_0} - Qt^{3/S} \right] \quad (1)$$

where t is the time after excitation, τ_0 is the intrinsic decay time of isolated donors in the absence of acceptors. The value of $S = 6, 8$ or 10 depends on whether the dominant mechanism of the interaction is dipole-dipole, dipole-quadrupole or quadrupole-quadrupole, respectively. Q is the energy transfer parameter which is defined by

$$Q = \frac{4\pi}{3} \Gamma \left(1 - \frac{3}{S} \right) C_A (C_{DA}^{(S)})^{3/S} \quad (2)$$

where $\Gamma \left(1 - \frac{3}{S} \right)$ is the gamma function, which is equal to 1.77 for dipole-dipole ($S = 6$), 1.43 for dipole-quadrupole ($S = 8$) and 1.30 for quadrupole-quadrupole ($S = 10$) interactions, respectively; C_A is the concentration of acceptors, which practically coincides with the total concentration of RE ions; $C_{DA}^{(S)}$ is the donor-acceptor interaction parameter, which is given by

where R_0 is the critical distance defined as a donor-acceptor separation for which the rate of energy transfer to the acceptors is equal to the rate of intrinsic decay of the donor.

The excitation energy can also migrate among donor ions until an acceptor ion is reached. If migration processes among donors are important, then according to the generalized Yokota-Tanimoto model (or Martin-Lavin model) [18, 19], the fluorescence decay intensity $I(t)$ is given by the function:

$$I(t) = I_0 \exp \left[-\frac{t}{\tau_0} - Qt^{3/S} \left(\frac{1+a_1X+a_2X^2}{1+b_1X} \right)^{(S-3)/(S-2)} \right] \quad (4)$$

where a_1, a_2 and b_1 are Padé approximate coefficients, which depend on the type of multipolar interaction and are given in Ref. [18, 19], $X = DC_{DA}^{-2/S} t^{1-2/S}$ and D is the diffusion coefficient which characterizes the energy migration processes between donors.

The non-exponential decay curves of the samples LaF_3 doped with 1.0; 3.0; 4.0 and 5.0 mol% Sm^{3+} are well fitted to IH model. Figure 6 shows the best fit of the experimental PL decay curve of $\text{LaF}_3:5\%\text{Sm}^{3+}$ sample to IH model (Eq. (1)) for $S = 8$ with $\chi^2 = 0.00017, R^2 = 0.99287$, using value $\tau_0 = 6.70$ ms obtained for 0.1 mol% Sm^{3+} concentration. The fits with $S = 6$ and 10 are also shown in Figure 6 for comparison. Thus, the best fits of the measured PL decay curves to IH model with $S = 8$ indicate that the dominant interaction for energy transfer of Sm^{3+} ions in $\text{LaF}_3:\text{Sm}^{3+}$ nanocrystals is dipole-quadrupole interaction. From the fits, the values of energy transfer parameter Q , critical distance R_0 , donor-acceptor interaction parameter C_{DA} are obtained and shown in Table 1. It can be seen from the table, the magnitude of Q increases from 0.3 to 1.92 with increasing Sm^{3+} concentration from 1.0 to 5.0 mol%. The same trend is observed in the case of R_0 (from 4.50 to 5.83 cm^{-8}) and C_{DA} (from 0.25×10^{-56} to $2.00 \times 10^{-56} \text{cm}^8/\text{s}$).

Using Judd-Ofelt theory [20], the predicted radiative lifetimes τ_R for ${}^4G_{5/2}$ level of Sm^{3+} ion in $\text{LaF}_3:3\%\text{Sm}^{3+}$, $\text{LaF}_3:4\%\text{Sm}^{3+}$ and $\text{LaF}_3:5\%\text{Sm}^{3+}$ samples have been calculated to be 3.81, 2.51 and 1.83 ms, respectively. For $\text{LaF}_3:1\%\text{Sm}^{3+}$ sample, because the absorption spectrum is too weak, the radiative lifetime cannot be calculated. As shown in Table 1, the experimental lifetime τ_{exp} for 593 nm emission line of $\text{LaF}_3:3\%\text{Sm}^{3+}$, $\text{LaF}_3:4\%\text{Sm}^{3+}$ and $\text{LaF}_3:5\%\text{Sm}^{3+}$ samples are determined to be 1.80, 1.16 and 0.75 ms, respectively, smaller than the calculated radiative lifetime τ_R . The discrepancy between calculated and experimental lifetimes can be attributed to non-radiative relaxation (multiphonon decay and energy transfer). The measured lifetime includes all relaxation processes (both radiative and non-radiative processes) and can be expressed as [20]

$$\frac{1}{\tau_{\text{exp}}} = \frac{1}{\tau_R} + W_{MP} + W_{ET} \quad (5)$$

where W_{MP} is the rate of multiphonon relaxation, W_{ET} is the

rate of energy transfer which often occurs through the cross-relaxation between pairs of the neighbouring RE ions. The W_{MP} is proportional to $\exp(-\frac{a\Delta E}{\hbar\omega})$, where a is a positive host-dependent constant, ΔE is the energy gap between the studied excited level and the next lower level and $\hbar\omega$ is the phonon energy of the host material [21, 22]. In the case of Sm³⁺ ion doped in LaF₃ nanocrystals, the energy gap ΔE between the ⁴G_{5/2} level and the next lower level ⁶F_{11/2} is approximately 6900 cm⁻¹ much larger than phonon energy of LaF₃ (350 cm⁻¹). Hence the multiphonon relaxation is negligible and the rate of energy transfer is given by

$$W_{ET} = \frac{1}{\tau_{exp}} - \frac{1}{\tau_R} \quad (6)$$

The luminescence quantum efficiency of the excited state η is equal to the ratio of the experimental lifetime to the radiative lifetime [20]:

$$\eta = \frac{\tau_{exp}}{\tau_R} \times 100\% \quad (7)$$

The values of W_{ET} and η for ⁴G_{5/2} level given in Table 1 show that the rate of energy transfer increases and quantum efficiency decreases with increasing of Sm³⁺ concentration.

It is worth noting that studying spectroscopic properties of Eu³⁺ ions doped in LaF₃ nanoparticles, Sudarsan and co-workers [23] have come to the conclusion that there are two types of Eu³⁺ ions in the LaF₃:Eu³⁺ lattice: the Eu³⁺ ions at the surface and the Eu³⁺ ions in the “bulk” (core) of the nanoparticles. In addition, the surface Eu³⁺ ions have a less symmetric crystal field than the “bulk” ones. When analyzing the PL decay curves for the oleic acid capped LaF₃:Eu³⁺ nanoparticles, Janssens and co-workers [7] have revealed that the effective PL lifetime τ_{eff} decreases with increasing Eu³⁺ concentration. This has been attributed to the increased Eu³⁺ to Eu³⁺ ion energy transfer and the non-radiative recombination at the surface. In our case of LaF₃:Sm³⁺ nanocrystals, the crystallite size decreases from 27 to 16 nm with increasing Sm³⁺ concentration from 0.0 to 5.0 mol%. Hence, the ratio between the number of the surface Sm³⁺ ions and that of the “bulk” Sm³⁺ ions for the LaF₃:5%Sm³⁺ nanocrystals is higher in comparison with the LaF₃ nanocrystals doped with lower Sm³⁺ concentrations. In that case, the excitation energy will be transferred from the “bulk” Sm³⁺ ions to the surface Sm³⁺ ions followed by non-radiative recombination at centers at the surface of nanocrystals. Just the phenomena including the Sm³⁺ to Sm³⁺ ion energy transfer and the non-radiative recombination at the surface are believed to lead to the decrease of the luminescence efficiency and lifetime of the ⁴G_{5/2} excited state when Sm³⁺ ion concentration increases as observed experimentally.

4. Conclusion

The undoped LaF₃ and LaF₃:Sm³⁺ nanocrystals have been synthesized hydrothermal method. The obtained nanocrystals possess hexagonal structure with $P\bar{3}c1$ space group. The characteristic PL and PLE spectra of Sm³⁺ ions doped in LaF₃

nanocrystals have been clearly observed. These spectra were interpreted by optical intra-configurational f–f transitions within Sm³⁺ ions. The PL decay curve of the LaF₃ sample doped with 0.1 mol% Sm³⁺ is found to be perfectly single-exponential, while the PL decay curves of the samples doped with 1.0; 3.0; 4.0 and 5.0 mol% Sm³⁺ are non-exponential. The reason for this is that when Sm³⁺ ion concentration in nanocrystals is increased, the excitation energy is transferred from the “bulk” Sm³⁺ ions to the surface Sm³⁺ ions followed by non-radiative recombination at centers at the surface of nanocrystals. The non-exponential behavior of the PL decay curves for LaF₃ nanocrystals doped with 1.0-5.0 mol% Sm³⁺ are well fitted to Inokuti-Hirayama model with the dominant dipole-quadrupole interaction. The values of fitting parameters for the energy transfer process were determined.

References

- [1] GuiLuo, Cui Xiaoxia, Wei Wei, Peng Bo, Fan Dianyuan, “Effects of different ligands on luminescence properties of LaF₃:Nd nanoparticles,” *J. Rare Earths.*, vol. 31, pp. 645-649, 2013.
- [2] Zhe Wang, Chenghui Liu, Yucong Wang, and Zhengping Li, “Solvent-assisted selective synthesis of NaLaF₄ and LaF₃ fluorescent nanocrystals via a facile solvothermal approach,” *J. Alloys Compd.*, vol. 509, pp. 1964-1968, 2011.
- [3] L. G. Jacobsohn, K. B. Sprinkle, C. J. Kucera, T. L. James, S. A. Roberts, H. Qian, E. G. Yukihiro, T. A. De Vol, J. Ballato, “Synthesis, luminescence and scintillation of rare earth doped lanthanum fluoride nanoparticles,” *Opt. Mater.*, vol. 33, pp. 136-140, 2010.
- [4] J. J. Velázquez, V. D. Rodríguez, A. C. Yanes, J. del-Castillo, J. Méndez-Ramos, “Down-shifting in Ce³⁺-Tb³⁺ co-doped SiO₂-LaF₃ nano-glass-ceramics for photon conversion in solar cells,” *Opt. Mater.*, vol. 34, pp. 1994-1997, 2012.
- [5] RuifeiQin, Hongwei Song, Guohui Pan, XueBai, Biao Dong, Songhai Xie, Lina Liu, Qilin Dai, XuesongQu, XinguangRen, and Haifeng Zhao, “Polyol-mediated synthesis of hexagonal LaF₃ nanoplates using NaNO₃ as a mineralizer,” *Cryst. Growth Des.*, vol. 9, pp. 1750-1756, 2009.
- [6] Cong-Cong Mi, Zhen-huangTian, Bao-fu Han, Chuan-bin Mao and Shu-kun Xu, “Microwave-assisted one-pot synthesis of water-soluble rare-earth doped fluoride luminescent nanoparticles with tunable colors,” *J. Alloys Compd.*, vol. 525, pp. 154-158, 2012.
- [7] S. Janssens, G. V. M. Williams, D. Clarke, “Systematic study of sensitized LaF₃:Eu³⁺ nanoparticles,” *J. Appl. Phys.*, vol. 109, pp. 023506-023515, 2011.
- [8] Ann M. Cross, P. Stanley May, Frank C. J. M. van Veggel, Mary T. Berry, “Dipicolinate sensitization of europium luminescence in dispersible 5%Eu:LaF₃ nanoparticles,” *J. Phys. Chem. C*, vol. 114, pp. 14740-14747, 2010.
- [9] Kentaro Fukuda, Noriaki Kawaguchi, SumitoIshizu, Takayuki Yanagida, ToshihisaSuyama, Martin Nikl, Akira Yoshikawa, “Crystal growth and scintillation characteristics of the Nd³⁺ doped LaF₃ single crystal,” *Opt. Mater.*, vol. 32, pp. 1142-1145, 2010.

- [10] Mingzhen Yao, Alan G. Joly, Wei Chen, "Formation and luminescence phenomena of $\text{LaF}_3:\text{Ce}^{3+}$ nanoparticles and lanthanide-organic compounds in dimethyl sulfoxide," *J. Phys. Chem. C*, vol. 114, pp. 826-831, 2010.
- [11] V. D. Rodríguez, J. Del Castillo, A. C. Yanes, J. Méndez-Ramos, M. Torres, J. Peraza, "Luminescence of Er^{3+} -doped nanostructured $\text{SiO}_2\text{-LaF}_3$ glass-ceramics prepared by the sol-gel method," *Opt. Mater.*, vol. 29, pp. 1557-1561, 2007.
- [12] Qiang Wang, Yumin You, Richard D. Ludescher, Yiguang Ju, "Syntheses of optically efficient $(\text{La}_{1-x-y}\text{Ce}_x\text{Tb}_y)\text{F}_3$ nanocrystals via a hydrothermal method," *J. Lumin.*, vol. 130, pp. 1076-1084, 2010.
- [13] J. Pichaandi, Frank C. J. M. van Veggel, Mati Raudsepp, "Effective control of the ratio of red to green emission in upconverting LaF_3 nanoparticles co doped with Yb^{3+} and Ho^{3+} ions embedded in a silica matrix," *Appl. Mater. Interfaces*, vol. 2, pp. 157-164, 2010.
- [14] Hoang Manh Ha, Tran Thi Quynh Hoa, Le Van Vu, Nguyen Ngoc Long, "Optical properties and Judd-Ofelt analysis of Sm^{3+} ions in lanthanum trifluoride nanocrystals," *J. Mater. Sci.: Mater. Electron.*, doi 10.1007/s10854-016-5603-1, 2016.
- [15] T. Suhasini, J. Suresh Kumar, T. Sasikala, Kiwan Jang, Ho Sueb Lee, M. Jayasimhadri, Jung Hyun Jeong, SoungSoo Yi, L. Rama Moorthy, "Absorption and fluorescence properties of Sm^{3+} ions in fluoride containing phosphate glasses," *Opt. Mater.*, vol. 31, pp. 1167-1172, 2009.
- [16] J. Suresh Kumar, K. Pavani, T. Sasikala, A. SreenivasaRao, Neeraj Kumar Giri, S. B. Rai, L. Rama Moorthy, "Photoluminescence and energy transfer properties of Sm^{3+} doped CFB glasses," *Solid State Sci.*, vol. 13, pp. 1548-1553, 2011.
- [17] M. Inokuti and F. Hirayama, "Influence of energy transfer by the exchange mechanism on donor luminescence," *J. Chem. Phys.*, vol. 43, pp. 1978-1989, 1965.
- [18] I. R. Martin, V. D. Rodriguez, U. R. Rodriguez-Mendoza, V. Lavin, E. Montoya and D. Jaque, "Energy transfer with migration. Generalization of the Yokota-Tanimoto model for any kind of multipole interaction," *J. Chem. Phys.*, vol. 111, pp. 1191-1194, 1999.
- [19] V. Lavin, I. R. Martin, C. K. Jayasankar, Th. Tröster, "Pressure-induced energy transfer processes between Sm^{3+} ions in lithium fluoroborate glasses," *Phys. Rev. B*, vol. 66, pp. 064207-064214, 2002.
- [20] C. Gorller-Walrand, K. Binnemans, in: K. A. Gschneidner, L. Eyring (Eds.), "Handbook on the Physics and Chemistry of Rare Earths," Elsevier – Publishing, Inc. New York, 1998, pp. 101.
- [21] T. Miyakawa and D. L. Dexter, "Phonon sidebands, multiphonon relaxation of excited states, and phonon-assisted energy transfer between ions in solids," *Phys. Rev. B*, vol. 1, pp. 2961-2969, 1970.
- [22] Jie Yang, Bin Zhai, Xin Zhao, Zhiqiang Wang, Hai Lin, "Radiative parameters for multi-channel visible and near-infrared emission transitions of Sm^{3+} in heavy-metal-silicate glasses," *J. Phys. Chem. Solids*, vol. 74, pp. 772-778, 2013.
- [23] V. Sudarsan, Frank C. J. M. van Veggel, Rodney A. Herring and Mati Raudsepp, "Surface Eu^{3+} ions are different than "bulk" Eu^{3+} ions in crystalline doped LaF_3 nanoparticles," *J. Mater. Chem.*, vol. 15, pp. 1332-1342, 2005.